Postharvest Biology and Technology 192 (2022) 112024

Contents lists available at ScienceDirect

Postharvest Biology and Technology

journal homepage: www.elsevier.com/locate/postharvbio

Blue light increases anthocyanin content and delays fruit ripening in purple pepper fruit

Ying Liu [a,b,*], Rob E. Schouten [a,c,*], Yury Tikunov [b], Xinxuan Liu [a,b], Richard G.F. Visser [b], Fei Tan [a], Arnaud Bovy [b], Leo F.M. Marcelis [a]

[a] Horticulture and Product Physiology, Wageningen University and Research, P.O. Box 16, 6700 AA Wageningen, the Netherlands
[b] Plant Breeding, Wageningen University and Research, P.O. Box 386, 6700 AJ Wageningen, the Netherlands
[c] Wageningen Food & Biobased Research, Wageningen University and Research, 6708 WG Wageningen, the Netherlands

ARTICLE INFO

Keywords:
Light spectrum
Light intensity
Anthocyanin biosynthesis
Anthocyanin degradation
Kinetic modelling

ABSTRACT

In purple-fruited *Capsicum* genotypes, fruit anthocyanin content first increases, and later decreases upon ripening. In this study, the response of this transient anthocyanin accumulation as a function of light intensity and light spectrum was investigated. Harvested fruit at the mature purple stage were illuminated by white-red LED lights at a photosynthetic photon flux density of 0 (darkness), 80, 160 and 320 μmol m^{-2} s^{-1} or illuminated by 24 (white light), 57%, 72% and 99% blue light (400–500 nm) at a photosynthetic photon flux density of 80 μmol m^{-2} s^{-1} for 28 d. Total anthocyanin, chlorophyll, capsanthin and soluble sugar contents, and their related gene expression, were measured. Anthocyanin content was hardly affected by white-red light intensity. Increasing the blue light fraction increased anthocyanin levels, via enhancing anthocyanin biosynthesis. This is supported by kinetic modelling and higher expression levels of the anthocyanin biosynthetic genes *CaMYB*, *CaCHS*, *CaDFR*, *CaANS* and *CaUFGT*. A higher blue light fraction delayed fruit ripening. This is supported by delayed sugar accumulation as indicated by kinetic modelling and transcriptome analysis. Transcriptome analysis indicated that 91% of the differentially expressed genes down-regulated during ripening had a higher expression in the 72% compared to 24% blue light treatment. In addition, PCA analysis of transcriptomic data indicated fruit ripening and senescence related genes *NCED1*, *NCED2*, *NOR* and *RIN* were expressed less in fruit illuminated by 72% blue light. Pathways upstream of ethylene production were downregulated in fruits illuminated with higher blue light fractions that might result in suppressed ethylene production. Higher fractions of blue light during postharvest storage might be applied to improve fruit anthocyanin levels but are not suited to create ripe anthocyanin rich pepper fruit.

1. Introduction

Peppers (*Capsicum* spp.) are colourful fruit with abundant phytochemicals such as chlorophyll, carotenoids, flavonoids and ascorbic acid. During development, fruit from most pepper genotypes turn from green to red. The main carotenoid responsible for the red colour of ripe pepper fruit is capsanthin (Hornero-Mendez et al., 2000; Howard et al., 2000). There are also pepper genotypes that produce an attractive purple fruit due to the formation of anthocyanins during fruit development. Anthocyanins are phytochemicals and potent antioxidants that form a subclass of polyphenolic flavonoids (Gould et al., 2002; Nakabayashi et al., 2014). Consumers prefer anthocyanin-rich food in their diets (Heber and Bowerman, 2001; Guidi et al., 2014) as anthocyanin-rich food has health-promoting properties (Sandoval-Ramírez et al., 2018; Igwe et al., 2019). The fading of purple colouration is affected by fruit ripening as only unripe fruit are purple, and their anthocyanin content decreases later in fruit development (Yamada et al., 2019).

Anthocyanin content is the net result of anthocyanin biosynthesis and degradation. The anthocyanin biosynthetic pathway has been elucidated and is conserved in many plants (Passeri et al., 2016; Liu et al., 2018a,b). Anthocyanin accumulation has been demonstrated to be affected by both light intensity and light spectrum (Zoratti et al., 2014). Light intensity affects anthocyanin content in fruit of several crops. For example, the sunlit peel of apple fruit accumulated more anthocyanin than the shaded peel (Feng et al., 2013). Domesticated tomato fruit do

* Corresponding authors at: Horticulture and Product Physiology, Wageningen University and Research, P.O. Box 16, 6700 AA Wageningen, the Netherlands
E-mail addresses: ying.liu@wur.nl (Y. Liu), rob.schouten@wur.nl (R.E. Schouten).

https://doi.org/10.1016/j.postharvbio.2022.112024
Received 25 April 2022; Received in revised form 31 May 2022; Accepted 25 June 2022
Available online 1 July 2022

not contain anthocyanins due to incomplete activation of its flavonoid pathway (Colanero et al., 2020). When an anthocyanin biosynthetic regulatory gene *BrTT8* was overexpressed in tomato (cv. Ailsa Craig), anthocyanins were produced in the epicarp at high light intensity, but not at low intensity (Zhang et al., 2019). Light spectrum may also affect anthocyanin content (Li and Kubota, 2009). For instance, blue light increased the anthocyanin content and the transcript level of anthocyanin biosynthetic genes more than white or red light in both attached and detached strawberry fruit (Kadomura-Ishikawa et al., 2013; Zhang et al., 2018). Several studies have shown that blue light outperforms other colours such as white and red lights in increasing anthocyanin content (Meng et al., 2004; Kadomura-Ishikawa et al., 2013; Tao et al., 2018; Zhang et al., 2018). Anthocyanin degradation has been shown in various tissues during plant development (Oren-Shamir, 2009). For instance, anthocyanin degradation can be observed in seedlings and young leaves (juvenile reddening) of many plant species (Chalker-Scott, 1999; Kubasek et al., 1992), in flowers of *Brunfelsia calycina* (fading) (Zipor et al., 2015) and in fruit of purple *Capsicum annuum* genotypes (Borovsky et al., 2004; Yamada et al., 2019). However, the mechanism of anthocyanin degradation is far less known. So far, peroxidases, polyphenol oxidases, laccases and ß-glucosidase have been reported to degrade anthocyanins in plants (Barbagallo et al., 2007; Fang et al., 2015; Zipor et al., 2015; Dong et al., 2019).

Our aim is to study the responses of pepper fruit to white-red light intensity and light quality of blue fraction, with regard to anthocyanin turnover and fruit ripening. During pepper fruit ripening, soluble sugar content increases (Rao et al., 2011), chlorophyll content decreases and carotenoid content increases (Howard et al., 2000; Russo and Howard, 2002; Borovsky and Paran, 2008). Here, pepper fruit harvested at the mature purple stage were illuminated by different intensities of white-red LED light or different fractions of blue LED light. We quantified anthocyanin content and the expression of anthocyanin biosynthetic genes during light treatments. Chlorophyll, capsanthin and soluble sugar contents were also measured as ripening indicators. In addition, we quantified transcript profiles (RNA-seq) of the two most contrasting white-red light intensities and of the two most contrasting blue light fractions. We also used kinetic modelling to test (i) whether anthocyanin biosynthesis or degradation was affected by the blue light fraction and (ii) how soluble sugar accumulation was affected by the blue light fraction. We show that white-red light intensity has a minor effect on the anthocyanin content and that the blue light fraction has a clear, ripening related, effect on anthocyanin biosynthesis.

2. Materials and methods

2.1. Fruit materials and experimental conditions

Bell pepper fruit of a purple-fruited cultivar, *Capsicum annuum* accession #3124, were harvested at the mature purple stage (four to five weeks after anthesis) from Sunrise Pepper Growers (Bleiswijk, the Netherlands). Fruit of this purple-fruited cultivar start to accumulate anthocyanins five to ten days after anthesis. Two experiments were conducted, one for the white-red light intensity (Exp-Int from Light **Int**ensity) and one for the blue light fraction (Exp-B from **B**lue Light) experiment. Pepper plants were cultivated in a greenhouse under standard Dutch commercial conditions. Fruit from batch 1 and batch 2, harvested on September 12th and November 6th 2018, respectively, were used for Exp-B. Fruit from batch 3 and batch 4, harvested on June 21st and August 28th 2019, respectively, were used for Exp-Int. Fruit were harvested and transported to our lab (d 0). Fruit were visually sorted to eliminate damaged and shrivelled fruit, and selected based on colour, size and uniformity. The selected fruit were surface sterilized with 70% (v/v) ethanol for two seconds, washed with demineralized water and tissue dried. The calyx of the fruit was covered with paraffin to seal both the wound and stomata in order to prevent water loss. The calyx was covered with aluminium foil to prevent light impact. Afterwards, fruit of the same batch were placed randomly in a vertical farming set-up with eight compartments (each an experimental unit) in a climate chamber. The sides of each compartment were covered with white plastic reflection films to prevent light leakage and to increase light uniformity. In each compartment, fruit were stored in two transparent plastic boxes (L55 *W40 *H 25 cm) covered with transmissive plastic lids illuminated by light emitting diodes (LEDs). To ensure that each fruit received the same light environment, fruit were turned upside down and randomized daily within each box.

For Exp-Int, a thermal stabilizer system was installed in each box to prevent variation in fruit temperature caused by variation in light conditions. This system consisted of a 5 cm water layer in the box, a pump and an aquarium heater. Thus, the air, water and fruit inside the box and air in the chamber were able to exchange heat flux with each other. The climate chamber was set to 13 °C with 85% relative humidity. The temperature setting of the aquarium heaters was based on the actual condition under different treatments to keep the fruit temperature between 20 and 21 °C. For Exp-B, the chamber temperature was set to 18 °C with 85% relative humidity. Here, a 5 cm layer of water was sufficient to keep the fruit temperature between 20 and 21 °C. Fruit temperature was measured by dataloggers with thermocouples attached to fruit on the non-illuminated side (k-type on TC-08 data loggers; Picotechnology LTD., Cambridge, UK). The thermocouples were shielded with aluminium foil to avoid direct LED light radiation. For both Exp-Int and Exp-B, the relative humidity in the box was above 95% (HM70, Vaisala, Finland) with ambient CO_2 levels. Fruit were placed in petri dishes on a white foam board to avoid water contact.

2.2. Light treatments and experimental set-up

In Exp-Int, white-red LED lighting (GreenPower LED production module 120 cm, DeepRedWhite, Signify, the Netherlands) was used to generate four light intensities, namely a photosynthetic photon flux density (PPFD) of 0 (darkness), 80, 160 and 320 μmol m^{-2} s^{-1}. In Exp-B, blue LEDs (GreenPower LED production module 120 cm, Blue, Signify, Netherlands) and white-red GreenPower LEDs (with all red LEDs blocked) were used to create varying fractions of blue light (400–500 nm; as percentage of PPFD), namely 24% (white light), 5 7%, 72% and 99% at the PPFD of 80 μmol m^{-2} s^{-1}. The PPFD was measured with a quantum sensor (LI-250A, LI-COR, USA) at fruit level by adjusting the height of the LED fixtures. The spectra were measured using a spectroradiometer (SS-110; Apogee Instruments, Logan, UT, United States). The treatments in the eight compartments (experimental units) were randomized for each fruit batch. The phytochrome photostationary state (PSS) values were calculated according to Sager et al. (1988). Both experiments lasted for 28 d with 24 h illumination per day. The experimental setups are summarized in Table 1.

2.3. Fruit sampling

Fruit were sampled at the start of the experiment (d 0) and subsequently every seven days until day twenty-eight. Each batch of fruit was sampled in the same way. At the start of the experiment, 16 fruit were selected randomly from one batch and pooled into eight replicates with two fruit per replicate. At d 7, 14, 21 and 28, four fruit per light treatment were randomly selected from two light compartments (one fruit per box) and pooled into two replicates, each with two fruit from the same light compartment. As anthocyanins are located in the peel of the fruit (Lightbourn et al., 2008), fruit peels were manually separated, immediately frozen in liquid nitrogen, grounded into powder (IKA, Germany) and stored at − 80 °C. The dry matter content of each sample was calculated based on the weight difference of 0.3 g frozen peel powder before and after freeze drying for three days.

Table 1
Overview of measured light conditions.

Experiment	Treatment	PPFD[a] (μmol m^{-2} s^{-1})	Blue[b] fraction[c] (%)	Green[b] fraction[c] (%)	Red[b] fraction[c] (%)	PSS[d]
White-red light intensity (Exp-Int)	Int-0	0	–	–	–	–
	Int-80	81.3 ± 0.4	11 ± 0.5	20 ± 0.3	69 ± 0.2	0.88
	Int-160	163.2 ± 1.2	11 ± 0.1	21 ± 0.4	68 ± 0.3	0.88
	Int-320	324.5 ± 2.9	11 ± 0.0	19 ± 0.1	70 ± 0.1	0.88
Blue light fraction (Exp-B)	B-24%	78.9 ± 1.0	24 ± 0.0	48 ± 0.1	28 ± 0.1	0.82
	B-57%	79.2 ± 1.0	57 ± 0.2	27 ± 0.4	16 ± 0.2	0.77
	B-72%	79.3 ± 0.5	72 ± 0.3	18 ± 0.1	10 ± 0.1	0.72
	B-99%	78.8 ± 0.6	99 ± 0.1	1 ± 0.1	0 ± 0.1	0.49

[a] PPFD, photosynthetic photon flux density (400–700 nm) measured at the fruit level. Values are the means ± s.e.m. of four light compartments of each treatment. The light intensity of each light compartment was based on 9 measurements equally distributed over the illuminated area in a box.
[b] Spectra: blue (400–500 nm), green (500–600 nm) and red (600–700 nm).
[c] Fractions are expressed as PPFD percentages.
[d] PSS, phytochrome photostationary state.

2.4. Anthocyanin extraction and determination

Anthocyanins were extracted and analysed according to Wahyuni et al. (2011) with some modifications. In brief, 0.3 g frozen peel powder was mixed with 700 μL 70% methanol containing 1% formic acid, vortexed and shaken for 30 min (Eppendorf thermomixer compact, Sigma-Aldrich, Germany). After centrifugation at 20,800 g for 10 min at room temperature, the extracts were filtered through a 0.45 μm PTFE membrane filter (Minisart® SRP4 Syringe Filter 17820). All extracts were determined by a liquid chromatography–mass spectrometry (LC-MS): Waters Acquity H-class Plus UPLC coupled to eλ Photo Diode Array with an Acquity QDa mass detector. Anthocyanins were separated on a Waters HSS T3 (150 ×2.1 mm, 2.1 μm) column at 35 °C using water (0.1% formic acid) as solvent A and acetonitrile (0.1% formic acid) as solvent B. The gradient was initially set at 95, 5% (A, B), then gradually went to 65, 35% (A, B) at 17 min, to 15, 85% (A, B) at 23 min and was kept constant for 1 min and then went to the initial settings. Quantification of anthocyanins was made at 520 nm using a calibration curve of an authentic standard of delphinidin chloride (Sigma-Aldrich).

2.5. Chlorophyll and capsanthin extraction and determination

Chlorophylls and carotenoids were extracted from 0.5 g frozen peel powder as described by Wahyuni et al. (2011) in darkness. In short, 4.5 ml MeOH/Chloroform (in the ratio 5–4) containing 0.1% (w/v) BHT was added to the frozen powder, vortexed and incubated on ice for 10 min. Then, 2.5 ml Tris-NaCl solution (50 mM, pH 7.5) was added to the mixture, vortexed and incubated on ice for 10 min. Two clear phases were formed by centrifuging the mixture at 720 g for 10 min (4 °C). The lower phase was collected and the upper phase was extracted twice with 1 ml chloroform containing 0.1% (w/v) BHT. The combined chloroform extracts were dried under a nitrogen flow. Dried extracts were stored in − 80 °C before HPLC analysis. Samples were re-dissolved in 1 ml ethyl acetate with 0.1% (w/v) BHT, sonicated for 10 min, centrifuged at 720 g for 1 min, filtered (0.45 μm PTFE membrane, Minisart® SRP4 Syringe Filter 17820) and transferred to dark brown vials (1.5 ml crimp neck vial 32 *11.6 mm amber glass, GBG® 11BW). Chlorophylls and carotenoids were separated and identified by a Waters HPLC (Alliance® e2695 Separations Module) coupled to a Waters 2996 photo diode array detector. Chromatographic separation was performed using a YMC30 (150 ×4.6 mm, 5 μm) column (YMC Co., LTD) at 35 °C using the following solvents: solvent A (80% methanol), solvent B (100% *tert*-butylmethyl ether) and solvent C (0.2% ammonium acetate). The gradient was initially set to 95, 0, 5% for A, B, C, respectively, from 0 to 12 min; then the ratio was instantly changed to 80, 15, 5% and gradually changed to 30, 65, 5% in 30 min and then kept constant for 10 min. Chlorophyll a, chlorophyll b and capsanthin were detected at 666 nm, 650 nm and 478 nm, respectively, and quantified using authentic standards for chlorophyll a, chlorophyll b and capsanthin. The highest chlorophyll a + chlorophyll b content and the highest capsanthin content of individual samples from each fruit batch were set to 1, respectively, and all measurements were expressed as relative content.

2.6. Carbohydrate extraction and determination

Soluble sugars were extracted according to Min et al. (2021) with some modifications. Namely, 15 mg freeze-dried peel powder was mixed with 5 ml 80% ethanol, vortexed, shaken in a water bath at 80 °C for 20 min and vortexed again. After centrifuge at 8500 g for 10 min (4 °C), 1 ml supernatant was vacuum dried at 50 °C and 5.1 mbar for 165 min (Savant SpeedVac SPD2010, Thermo Fisher Inc., Waltham, MA, United States), and then 1 ml Milli-Q water was added to redissolve the carbohydrates using an ultrasonic water bath for 10 min at room temperature. After centrifuging at 25,000 g for 15 min (4 °C), the solution was diluted 20 times with Milli-Q water for determination of soluble sugars (glucose, fructose and sucrose). Soluble sugars were quantified using a high-performance anion exchange chromatography with pulsed amperometric detection (HPAEC-PAD; Dionex™ ICS-5000, Thermo Fisher Scientific) and a Dionex™ CarboPac™ PA1 column (2 ×250 mm; Thermo Fisher Scientific) and eluted with 100 mM NaOH at a flowrate of 0.25 ml min^{-1} at 25 °C.

2.7. Fruit weight loss

Fruit fresh weight (FW) was measured at d 0 and at each sampling day. Fruit weight loss over time was expressed as percentage of the initial weight.

2.8. RNA extraction

Total RNA was extracted from the same peel powder as those used for metabolic analysis. RNA was isolated using a Plant RNA/DNA Purification Kit (Norgen Biotek Corp; E4788 Sigma-Aldrich) following the manufacturers' instructions. Any DNA contamination was removed by On-Column DNase I Digestion Set (Sigma-Aldrich). The purity and quantity of RNA was measured by a spectrophotometer (Nanodrop™ One Microvolume UV-Vis Spectrophotometer, Thermo Scientific™) and assessed by electrophoresis on a 1.5% w/v agarose gel using 200 ng of RNA. The A260/A280 and A260/A230 ratios of the samples were higher than 1.8. Samples with two clearly visible rRNA bands (1.1kB and 700 bp band) and no mRNA smear as well as the same brightness were qualified.

2.9. Quantitative real-time-PCR analysis (qRT-PCR)

Total RNA was reversely transcribed to cDNA using the Taqman® Reverse Transcription Reagent kit (Life Technologies, Applied Biosystems #N8080234) according to manufacturer's guidelines.

Expression levels of anthocyanin biosynthetic genes: *CaMYB* (CA10g11690), *CaCHS* (CA05g17060), *CaDFR* (CA02g22270), *CaANS* (CA01g03670) and *CaUFGT* (CA10g16530) were examined by qRT-PCR. The qRT-PCR was performed in a C1000 Touch™ Thermal Cycler (Bio-Rad CFX96™ Real-Time System, USA) with an iQ™ SYBR Green Supermix kit (Bio-Rad, USA). Gene specific primers were designed using Primer3Plus (http://www.bioinformatics.nl/cgi-bin/primer3plus/primer3plus.cgi). Three *ubiquitin* genes (AY486137, CA07g13540 and CA08g18230) were used as internal reference genes to correct gene expression. All primers used in this study are listed in Table S1. Each qPCR experiment was carried out in four biological replicates, with two technical replicates each. The reaction efficiency of qRT-PCR and R values were evaluated by LinRegPCR program (Ramakers et al., 2003), resulting in a range of 1.8–2.1 (efficiency) and 0.99–1.00 (R value). The Ct values were read under default conditions, and when the amplification signal was not detected by the qRT-PCR machine, the Ct value was given a value of 40 for calculation. The relative gene expression (RGE) level was calculated by $2^{-\Delta Ct}$ method (Livak and Schmittgen, 2001).

2.10. RNA-seq analysis

RNA extraction was described above; the RNA concentration was measured by Qubit® 2.0 Fluorometer (Invitrogen) using Qubit™ RNA BR Assay Kit (Invitrogen). The RNA-seq library was constructed using total RNA from four replicates of Int-0, Int-320, B-24% and B-72% on d 21 using Next-Generation Illumina sequencing (Bioscience, Wageningen University and Research, Netherlands). The clean reads were mapped to the *C. annuum* genome (Zunla v2.0, SOL Genomics Network database) using CLC Genomics Workbench 20 (CLC bio, Aarhus, Denmark) and the number of mapped reads for the genes were normalized to RPKM (reads per kilobase per million mapped reads). Genes with a highest RPKM value smaller than 5 were removed. Expression levels for all pepper genes were presented as RPKM + 1.9 (percentile 0.05%) and are summarized in Table S2. Differential expressions between B-72% and B-24% and between Int-320 and Int-0 were analysed with a DESeq2 R package (1.26.0). The raw p-values were corrected according to the Benjamini-Hochberg approach to determine the false discovery rate (FDR) for each gene. Genes with a false discovery rate (FDR) < 0.05 and an absolute value of the $\log_2$ fold change ($\log_2$FC) > 0.5 were designated as significantly differentially expressed genes (DEGs). DEGs are summarized in Table S3.

The protein sequences of the pepper DEGs were used as query to identify *Arabidopsis thaliana* homologs (TAIR10 version) by blastp. The Gene Ontology (GO) enrichment analysis was done by submitting obtained *Arabidopsis thaliana* homologs to agriGO v2.0 (http://systemsbiology.cau.edu.cn/agriGOv2/) and analysing them using Singular Enrichment Analysis (SEA) tool (Du et al., 2010; Tian et al., 2017). The Kyoto Encyclopedia of Genes and Genomes databases (KEGG) enrichment analysis was conducted using up-regulated and down-regulated pepper DEGs, respectively, as the foregrounds and the entire *Capsicum annuum* genes as the background. The online KEGG Orthology Based Annotation System (KOBAS; http://kobas.cbi.pku.edu.cn/kobas3) was used to test the enrichment of DEGs in the KEGG pathways (Xie et al., 2011). GO terms and KEGG pathways with corrected p-values < 0.05 were considered significantly enriched by DEGs.

2.11. Statistical analysis

The Exp-Int and Exp-B were each carried out as completely randomized block design. As for each fruit batch, the experiment was conducted with eight independent experimental units comprising two repetitions of four treatments in a climate chamber; a batch was considered as a block. In total, there are four statistical replicates in Exp-Int and Exp-B, with two blocks and two statistical replicates per block. A statistical replicate consisted of a pool of two fruit. One-way analysis of variance (ANOVA) was applied ($P < 0.05$) to test the light treatment effects on anthocyanin, chlorophyll, capsanthin, total soluble sugar (glucose, fructose and sucrose), weight loss and gene expression when comparing different treatments per day. Normality and homogeneity of residuals of the variables were tested by the Shapiro-Wilk test and the Bartlett's test, respectively. When necessary, data were log-transformed and the tests on residuals were repeated. If log-transformed data did not fulfil the ANOVA assumptions, the Kruskal-Wallis test was used to analyse the original non-transformed data. For multiple comparison tests, Fisher's protected LSD was conducted following ANOVA at the 0.05 level. Most statistical analyses were performed using Genstat (19th Edition, VSN International Ltd., Hemel Hempstead, UK) and the Kruskal-Wallis test was performed using Rstudio (Version 1.2.5033, USA).

2.12. Anthocyanin and total soluble sugars kinetic models

Two kinetic models were constructed. Kinetic models decompose the complex behaviour into simpler constituent processes and then describe those in terms of differential equations (Tijskens and Schouten, 2014). The first model described the total anthocyanin behaviour, the second model described the total soluble sugar content, both to investigate blue light fraction effects. The anthocyanin model is based on a simplified consecutive mechanism assuming that anthocyanins (in mg g^{-1} DW) are produced from a pool of precursors (in mg g^{-1} DW) with k_s (in d^{-1}) the rate constant of anthocyanin synthesis (Eq. (1)). Anthocyanins are assumed to be completely broken down (to nil) with rate constant k_d (in d^{-1}) (Eq. (2))

$$\text{Precursors} \xrightarrow{k_s} \text{Anthocyanins} \tag{1}$$

$$\text{Anthocyanins} \xrightarrow{k_d} \text{nil} \tag{2}$$

The model can be presented mathematically as a set of ordinary differential equations, based on the rules of chemical kinetics with the following analytical solution (Eq. (3)), showing anthocyanin behaviour over time (t), expressed as a combination of rate constants (k_s, k_d) and content of precursors at start of the experiment (d 0) ($Precursors_0$) and anthocyanins ($Anthocyanins_0$), respectively.

$$Anthocyanins(t) = Precursors_0 \quad \frac{k_s}{k_d - k_s}\left(e^{-k_s t} - e^{-k_d t}\right) + Anthocyanins_0 \quad e^{-k_d t} \tag{3}$$

The sugar model is based on observed sigmoidal behaviour that is often described by a logistic function (Schouten et al., 2007; Tijskens et al., 2017) that assumes that total soluble sugars (TSS in mg g^{-1} DW), are produced over time from a minimum content (TSS_{min} in mg g^{-1} DW) to a maximum content (TSS_{max} in mg g^{-1} DW) with rate constant k_{tss} (in d^{-1}) and *shift* (in d) (Eq. (4)). *shift* is a variable that indicates the stage of development of a batch, as indicated by the number of days past the midpoint of the logistic function.

$$TSS(t) \quad = TSS_{min} + \frac{(TSS_{max} - TSS_{min})}{1 + \quad e^{(-k_{tss} \quad (TSS_{max} - TSS_{min})(t + shift))}} \tag{4}$$

The equations of the model formulations were developed using Maple 2017 (MapleSoft, Waterloo Maple Inc., Waterloo, Canada). The models were implemented assuming that the measured anthocyanin and total soluble sugar over time are directly related to Eqs. (3) and (4), respectively. Data were analysed using an indexed version of the nls (non-linear regression) procedure of R (R Development CoreTeam, 2021) that allows assigning variation in the experimental data to specific sources. The variation in the data was assigned either per light treatment, per batch or in common for all fruit.

3. Results

3.1. White-red light intensity effects on fruit colour and metabolites

To examine the impact of white-red light intensity on the content of anthocyanins and other ripening associated metabolites, purple pepper fruit were illuminated by 0 (Int-0), 80 (Int-80), 160 (Int-160) and 320 (Int-320) μmol m^{-2} s^{-1} white-red LED lights for four weeks. We first estimated the effect of white-red light intensity on visually assessed fruit colour. Fruit gradually turned from dark purple to red during illumination with no clear indication of light intensity effects at each sampling day, except for those in Int-0 which showed shades of green after three weeks (Fig. 1 A). This, however, did not fully correspond with anthocyanin content. On d 7, the anthocyanin content was the highest in Int-0 fruit and the lowest in Int-160 fruit compared to both Int-80 and Int-320 fruit (Fig. 1B). Afterwards, the anthocyanin content did not significantly vary between different intensities, except that fruit in Int-320 showed lower anthocyanin content at d 21 and 28 compared to the other treatments. The transcript abundance of anthocyanin biosynthetic genes were also hardly affected (Fig. S1). This indicated that the overall effects of white-red light intensity on anthocyanin content were rather small.

Chlorophyll content decreased over time (Fig. 1C). At d 7, there was no significant difference in chlorophyll content among treatments. Later, Int-0 fruit had a significantly higher chlorophyll content than illuminated fruit which all showed similar chlorophyll content. Capsanthin and total soluble sugar contents increased over time. At d 14 and afterwards, there were significant differences in capsanthin content among treatments (Fig. 1D). Int-0 fruit had the lowest capsanthin content and Int-320 fruit had the highest capsanthin content at most sampling days. Total soluble sugar content was significantly lower in Int-0 fruit than in illuminated fruit after d 7 and it was similar between illuminated fruit with different white-red intensities (Fig. 1E). Glucose and fructose contents dominated total soluble sugar content (97 ± 0.3%) and their trends were similar as that of total soluble sugars (Fig. S2A&B). The sucrose content was low (3 ± 0.3%) (Fig. S2C). Fruit weight loss increased over time; the higher the light intensity, the higher the weight loss (Fig. 1 F).

3.2. Blue light effects on fruit colour and metabolites

3.2.1. Fruit colour and metabolite contents

To study the effect of blue light on anthocyanin content of purple pepper fruit, purple pepper fruit were illuminated by 24 (B-24%), 57 (B-

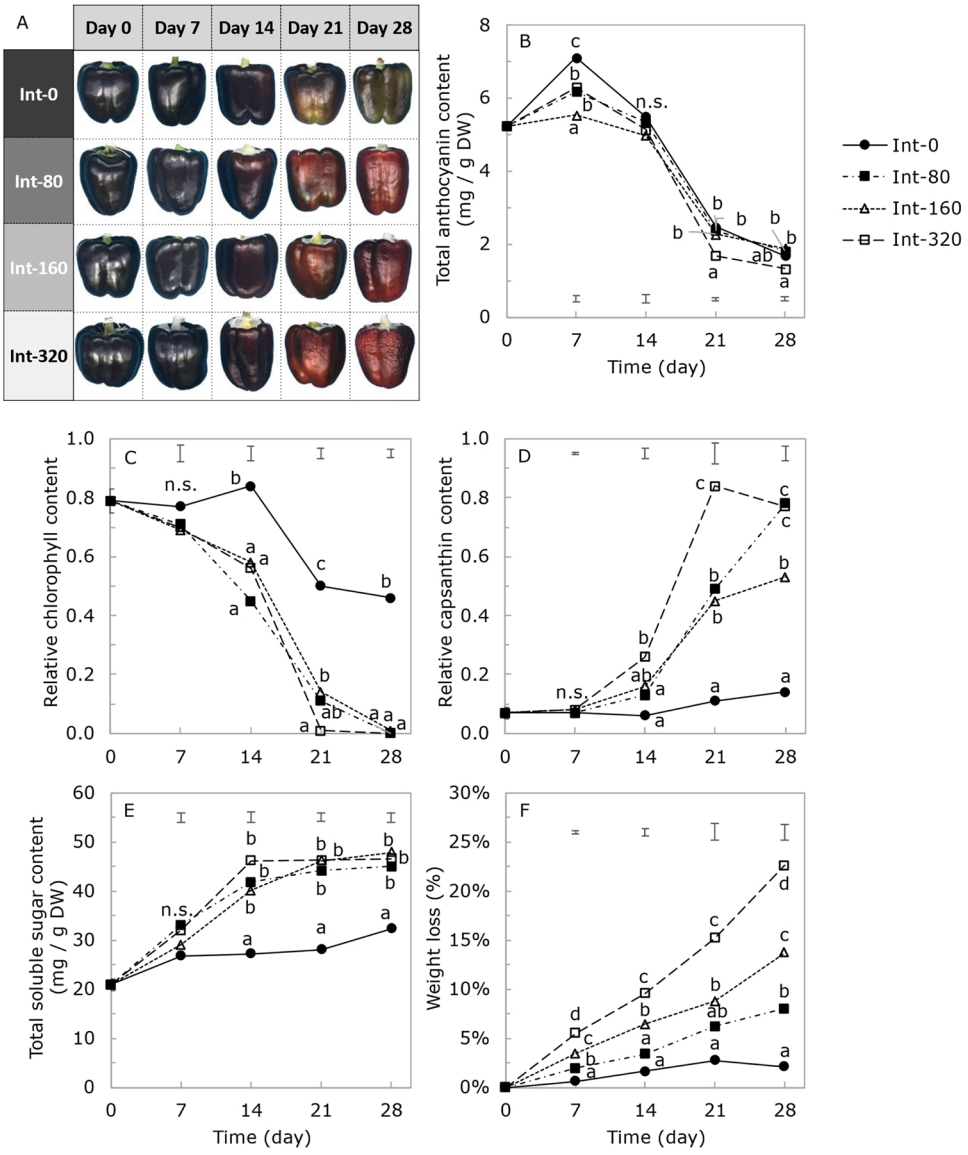

Fig. 1. Effects of illuminating pepper fruit by four white-red light intensities (0, 80, 160 and 320 μmol m^{-2} s^{-1} white-red LED lighting) on (A) fruit peel colour, (B) total anthocyanin content (mg g^{-1} DW), (C) relative chlorophyll content; (D) relative capsanthin content, (E) total soluble sugar content (mg g^{-1} DW) (glucose + fructose + sucrose) and (F) weight loss (in %) that were measured every seven days over a period of twenty-eight days. Error bars represent standard error of d 0 (n = 16) and standard error of means of d 7–28 (two batches as block with each two replicates, in total n = 4) from one-way ANOVA. ANOVA is not performed for data of d 0 because there is no treatment. Different letters indicate significant differences ($P < 0.05$) on the same day according to Fisher's Protected LSD; n.s. represents no significant differences.

57%), 72 (B-72%) and 99% (B-99%) blue light (400–500 nm) at 80 μmol m^{-2} s^{-1} for four weeks (Exp-B). Pepper fruit gradually turned from dark purple to red over time. The higher the blue light fraction was, the slower the fruit lost purple colour (Fig. 2 A). Anthocyanin content of B-24% fruit continuously decreased. Anthocyanin content of the other treatments first increased until d 7 and then gradually decreased afterwards (Fig. 2B). The anthocyanin content of B-72% fruit was the highest at d 7 and d 14. Anthocyanin content of B-99% fruit was the highest at the end of the experiment. Chlorophyll content of B-24% decreased continuously over time. Chlorophyll content of B-57%, B-72% and B-99% fruit first increased until d 7 and then gradually decreased (Fig. 2 C), similar to the trend in the anthocyanin accumulation. Capsanthin content increased as time progressed without showing significant differences between treatments (Fig. 2D). Total soluble sugar contents (glucose + fructose + sucrose) over time showed sigmoid behaviour. Total soluble sugar content of B-24% fruit was higher than that of fruit in other three treatments at d 14. Total soluble sugar content of B-72% and B-99% fruit was lower at d 21 compared to B-57% fruit. Glucose and fructose contents dominated total soluble sugar content (96 ± 0.3%) and their trends were similar to that of total soluble sugars (Fig. S3A&B). Sucrose content was low (4 ± 0.3%) and not influenced by the blue light fraction (Fig. S3C). Fruit gradually showed increasing weight loss over time without showing significant differences between treatments (Fig. 2 F).

3.2.2. *Modelling anthocyanin content*

The anthocyanin analytical solution (Eq. 3) was applied to describe all measured anthocyanin data for Exp-B to investigate whether blue light fraction affects the anthocyanin production; i.e. the rate constant of anthocyanin synthesis (k_s), the anthocyanin degradation; i.e. the rate constant of anthocyanin degradation (k_d), or both, in one joint parameter estimation. Initial and kinetic parameters were estimated with small standard deviations and highest variance explained for (R^2_{adj}) when k_s was estimated per blue light treatment, and k_d in common. A lower model performance was reached when other options (k_d estimated per light treatment with k_s in common, or both k_s and k_d estimated per light treatment) were explored. The variation in the parameter values estimations declined drastically when the initial parameters were estimated per fruit batch. The model was able to fit the data with a percentage variation accounted for (R^2_{adj}) of 90.5%. Anthocyanin content over time per batch is shown in Fig. 3 with the corresponding simulations calculated from the estimated parameters listed in Table 2. The results from this modelling approach indicate that the blue light fraction affects the anthocyanin synthesis rate, with the highest anthocyanin synthesis rate

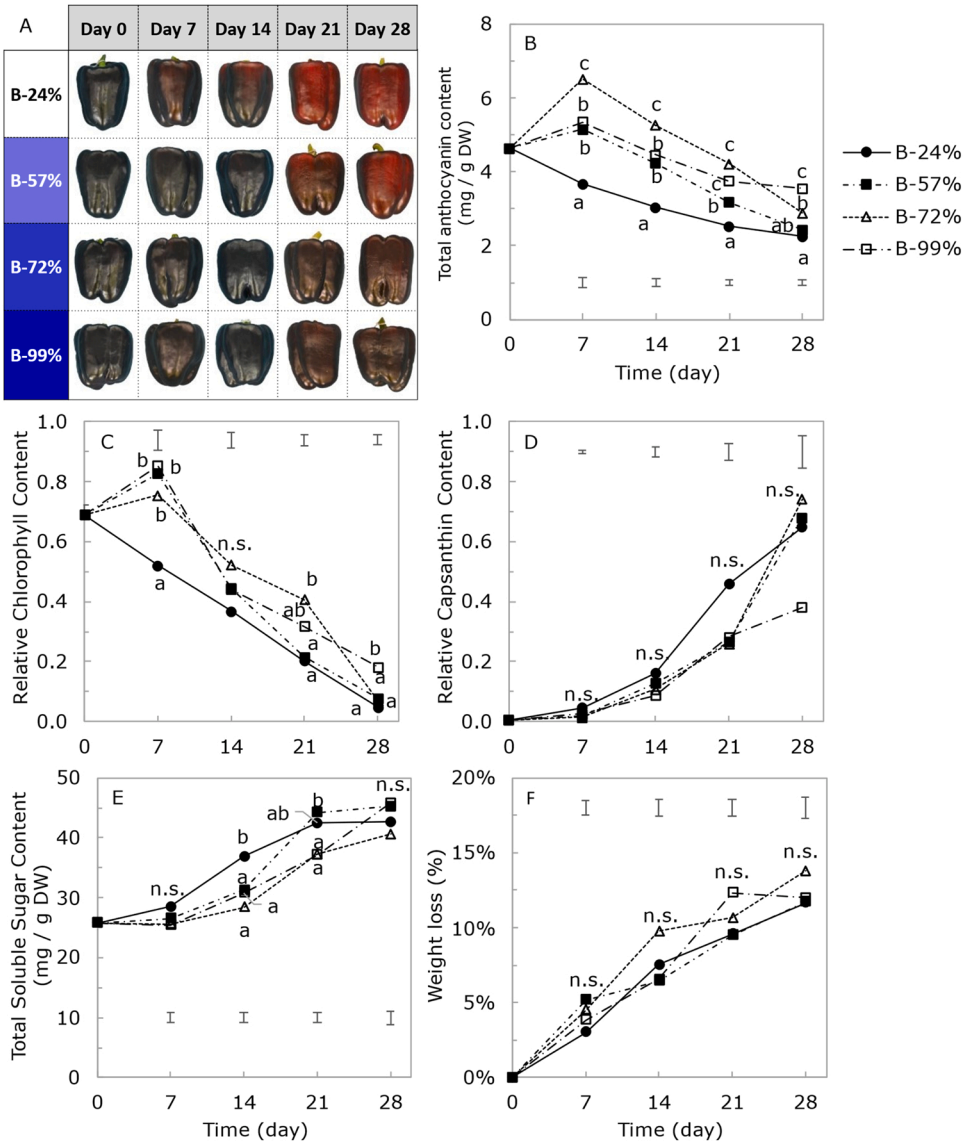

Fig. 2. Effects of illuminating pepper fruit by 24, 57%, 72% and 99% of blue lights (400–500 nm) at a total intensity of 80 μmol m^{-2} s^{-1} on (A) fruit peel colour, (B) total anthocyanin content (mg g^{-1} DW), (C) relative chlorophyll content; (D) relative capsanthin content, (E) total soluble sugar content (mg g^{-1} DW) (glucose + fructose + sucrose) and (F) weight loss (in %) that were measured every seven days for twenty-eight days. Error bars represent standard error of d 0 (n = 16) and standard error of means of d 7–28 (two batches as block with each two replicates, in total n = 4) from one-way ANOVA. ANOVA is not performed for data of d 0 because there is no treatment. Different letters indicate significant differences ($P < 0.05$) on the same day according to Fisher's Protected LSD; n.s. represents no significant differences.

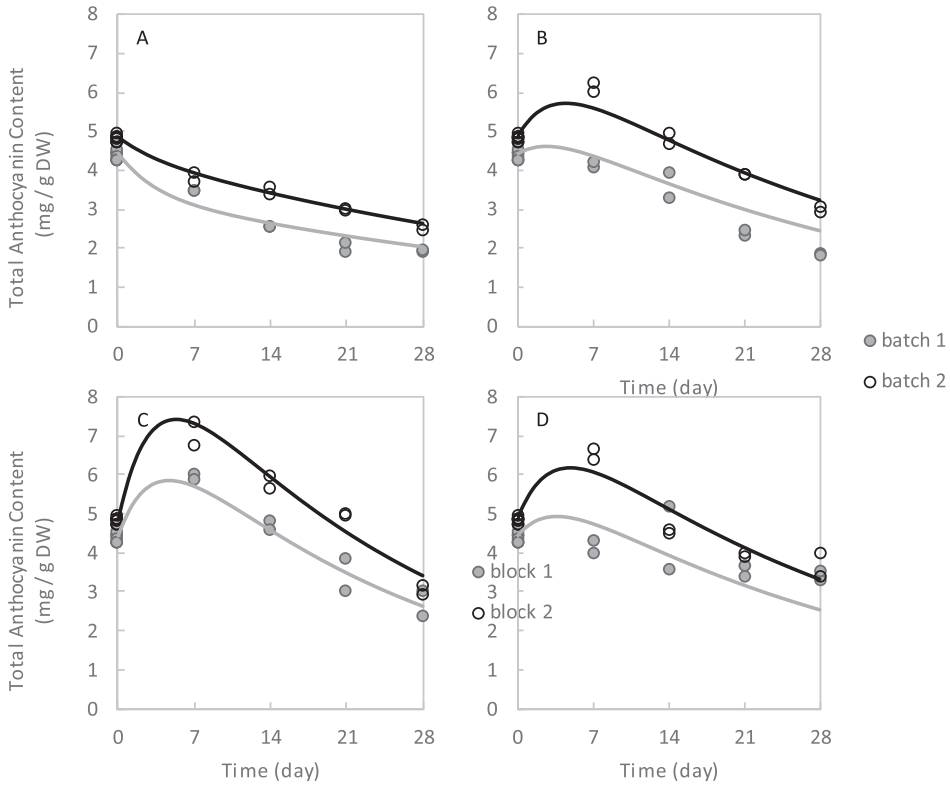

Fig. 3. Total anthocyanin content over time either as measured values (symbols) or with simulated model behaviour (lines) per fruit batch per light treatment: (A) 24% blue light, (B) 57% blue light, (C) 72% blue light and (D) 99% blue light.

Table 2
Overview of initial parameter estimates per fruit batch and estimated common kinetic parameters with indicated standard deviation of the anthocyanin model (Eq. 3).

	Units	Batch	Estimate	St.dev.
k_s *B-24%*	d^{-1}		0.018	0.001
k_s *B-57%*	d^{-1}		0.029	0.002
k_s *B-72%*	d^{-1}		0.040	0.004
k_s *B-99%*	d^{-1}		0.032	0.003
k_d	d^{-1}		0.30	0.09
$Precursor_0$	mg g^{-1} DW	1	53	20
	mg g^{-1} DW	2	69	26
$Anthocyanin_0$	mg g^{-1} DW	1	4.43	0.06
	mg g^{-1} DW	2	4.85	0.06

(k_s) for fruit in B-72%, but does not affect the degradation rate (k_d).

3.3. The effect of blue light fraction on the expression of anthocyanin biosynthetic genes

Anthocyanin biosynthesis was quantified by measuring the relative gene expression levels of anthocyanin biosynthetic genes. *CaMYB* (CA10g11690, homolog of tomato *SlAN2*(*SlMYB75*) (Kiferle et al., 2015; Jian et al., 2019)) encodes an R2R3-MYB transcription factor that activates the expression of anthocyanin structural genes. *CaCHS* (CA05g17060) is an early structural gene that belongs to the common flavonoid pathway. *CaDFR* (CA02g22270), *CaANS* (CA01g03670) and *CaUFGT* (CA10g16530) are three late structural genes. *CaDFR* diverts the common flavonoid pathway towards the anthocyanin biosynthetic pathway (Liu et al., 2020), where *CaANS* and *CaUFGT* are included. Although the expression level of *CaMYB* continuously declined in four treatments, it was significantly higher expressed in B-72% and B-99% fruit than in B-24% and B-57% fruit at d 7 (Fig. 4 A). *CaCHS* in B-72% or B-99% fruit had the highest expression level at d 7 and 21 (Fig. 4B). The expression levels over time of *CaDFR*, *CaANS* and *CaUFGT* showed similar trends to that of *CaMYB* (Fig. 4C-E). In addition, the expression levels of all anthocyanin biosynthetic genes from four treatments were significantly correlated at d 7 (Fig. S5). Thus, the longer retention of anthocyanins in fruit exposed to higher fractions of blue light might be due to a higher expression of the anthocyanin biosynthetic genes. This, however, does not exclude the possibility that hypothetical anthocyanin breakdown genes could also be downregulated by higher blue fractions. Since no anthocyanin degradative gene has been identified in pepper yet, a targeted gene expression analysis was not feasible. Therefore, a transcriptomic analysis of fruit from B-24% and B-72% on d 21 was performed using RNA-seq to further explore the transcriptional effect of blue light fractions. These fruit were selected based on their clear differences in anthocyanin content and ripening status. In total, 384 significantly differentially expressed genes (DEGs) were obtained, including 238 up-regulated DEGs and 146 down-regulated DEGs in B-72% fruit compared to B-24% fruit. Volcano plots for all genes and a hierarchical clustering heatmap for DEGs are shown in Fig. S4. A GO enrichment analysis was performed for all DEGs, and a KEGG pathway enrichment analysis was performed for up- or down-regulated DEGs, respectively. Among the top 10 enriched Biological Process GO terms, three GO terms relevant to anthocyanin biosynthesis were significantly enriched, namely the “phenylpropanoid biosynthetic process”, the “flavonoid biosynthetic process” and the “phenylpropanoid metabolic process”(Fig. 5 A). Among the top 20 enriched KEGG pathways, “flavonoid biosynthesis” and “phenylpropanoid biosynthesis” were significantly up-regulated in B-72% fruit compared to B-24% fruit, with “flavonoid biosynthesis” the greatest enriched pathway (Fig. 5B). Most of the down-regulated KEGG pathways were related to primary metabolism of amino acids, sugars and lipids.

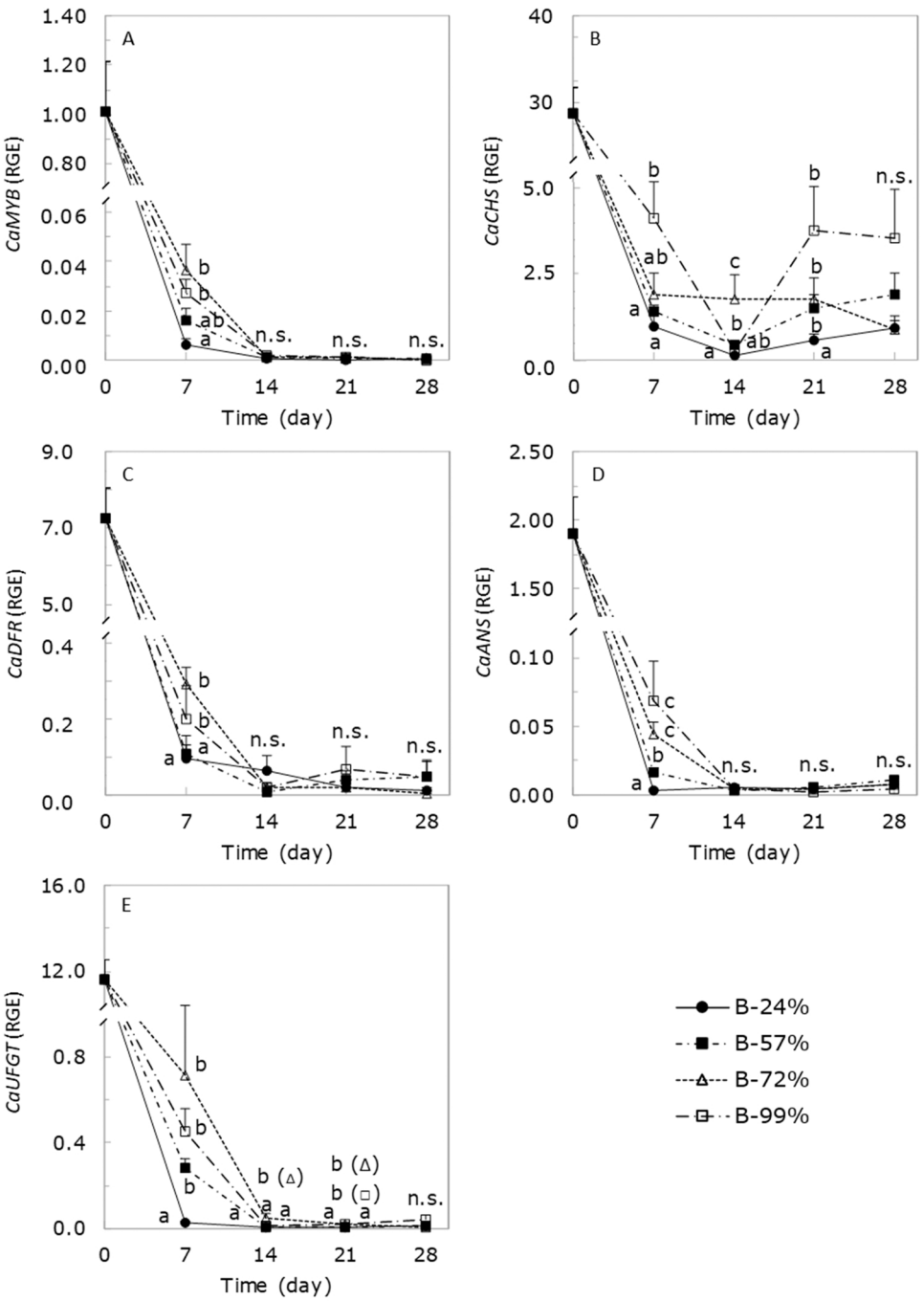

Fig. 4. The relative gene expression (RGE) level of (A) *CaMYB*, (B) *CaCHS*, (C) *CaDFR*, (D) *CaANS* and (E) *CaUFGT* in pepper fruit illuminated by 24, 57%, 72% and 99% blue light in Exp-B measured every seven days over twenty-eight days. Error bars represent standard error of d 0 (n = 16) and d 7 - d 28 (n = 4). One-way ANOVA is performed based on $\log_2$RGE values per day, from d 7 to d 28 (two batches as block with each two replicates, in total n = 4). ANOVA is not performed for data of d 0 because there is no treatment. Different letters indicate significant differences ($P < 0.05$) on the same day according to Fisher's Protected LSD; n.s. represents no significant differences.

3.4. The effect of blue light fraction on fruit ripening

3.4.1. Modelling total sugar content

The sugar model (Eq. (4)) was applied to describe the total soluble sugar (TSS) content for Exp-B to investigate whether blue light fraction affected the sugar accumulation, either by the rate constant k_{tss}, the minimum TSS content (TSS_{min}), the maximum TSS content (TSS_{max}) or the stage of development (*shift*). All scenarios were tested, assigning light treatment effects to k_{tss}, TSS_{min}, TSS_{max} or *shift*, separately or in combination. The highest percentage explained variation ($R^2_{adj} = 83.5\%$) was achieved when the light treatments were assigned to *shift* and estimated per batch. TSS content over time per batch is shown in Fig. 6A-B with the corresponding simulations calculated from the estimated parameters listed in Fig. 6 C. The results from this modelling approach showed that blue light illumination affected the *shift* parameter similarly per batch, indicating that blue light illumination affected the stage of fruit development. Fruit in B-72% consistently started later with sugar accumulation, i.e. were less ripe, while fruit in B-24% started earlier with sugar accumulation, i.e. were more ripe. Positive correlations between anthocyanin biosynthetic rate k_s and *shift* per batch were observed, indicating that fruit with a higher rate of anthocyanin synthesis were less ripe (Fig. 6D).

3.4.2. Transcriptome analysis for the effects of different blue light fractions on ripening related genes

Ripening correlation coefficients (RCC) were calculated by correlating the FPKM (Fragments Per Kilobase Million) of RNA-seq data from PepperHub (Liu et al., 2017) with days after flowering (Table S6). Genes

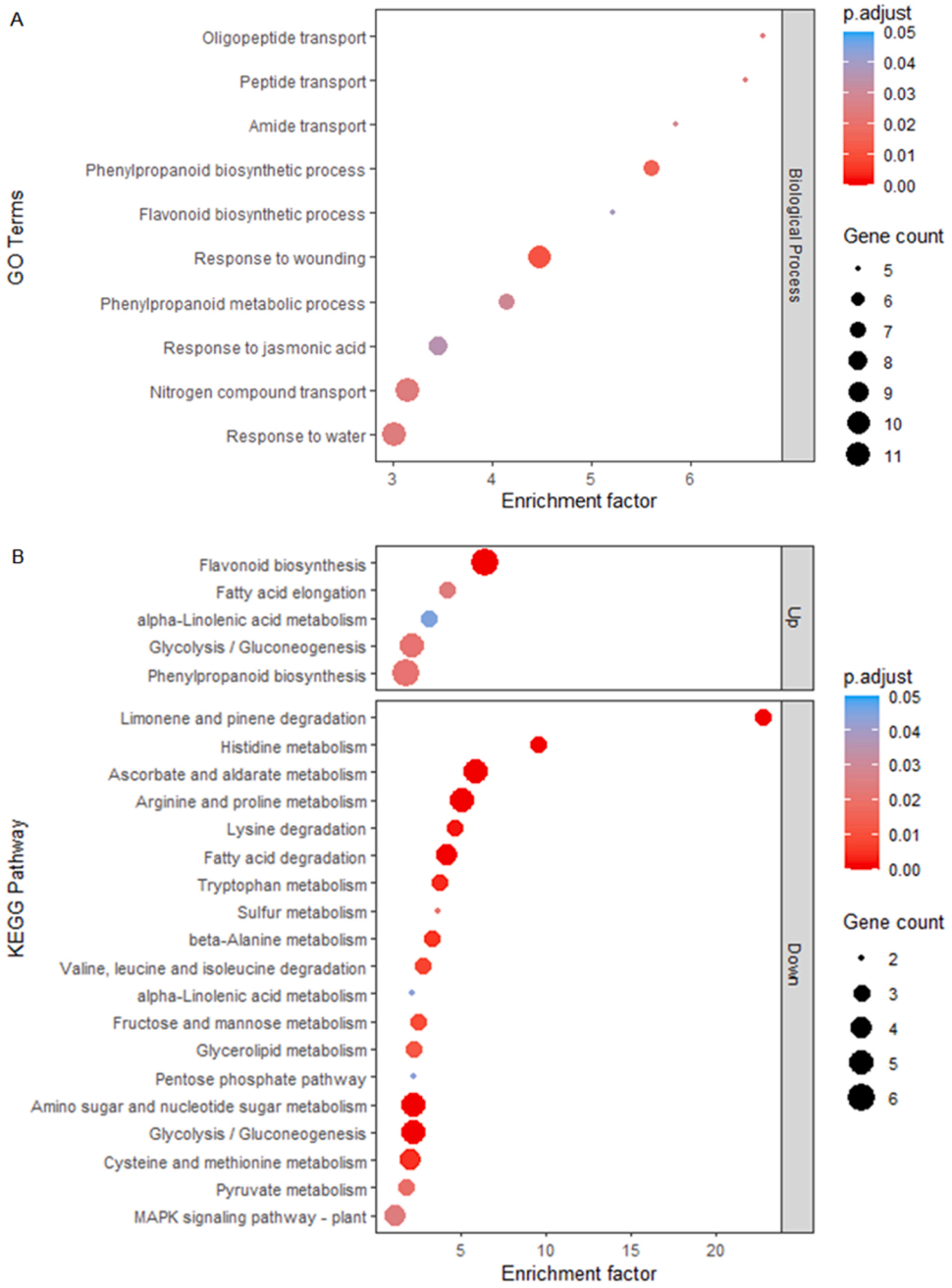

Fig. 5. Gene ontology (GO) enrichment analysis and KEGG pathway enrichment analysis. (A) Top 10 enriched biological process GO terms for all DEGs when comparing B-72% to B-24% at d 21. (B) KEGG enrichment analysis of up- and down-regulated DEGs in B-72% fruit compared to B-24% fruit at d 21, respectively. The vertical coordinate shows the significantly enriched GO terms/KEGG pathways, and the horizontal coordinate shows the enrichment factors (functionally-related groups of the genes in DEGs relative to in the genome background). The size of each point represents the number of genes in the pathway, and the colour of the point represents the adjusted *p*-value. A complete list of enriched GO terms and KEGG pathways is available in Tables S4 and S5.

with RCC < -0.5 and > 0.5 were considered as ripening dependent: RCC < -0.5 down-regulated during ripening and RCC > 0.5 up-regulated during ripening. The expression of 63% of DEGs were considered as ripening dependent. To estimate the effect of blue light fractions on the expressions of the ripening dependent DEGs, the $\log_2$FC of all DEGs were plotted versus their corresponding RCCs (Fig. 7). Among the DEGs that were considered down-regulated during ripening based on their RCC, 91% had a higher expression in B-72% fruit compared to B-24% fruit (Fig. 7). About 68% of ripening induced DEGs had lower expression levels in B-72% fruit compared to B-24% fruit.

3.5. *Blue light fraction differentially affected the expression of flavonoid and ripening related genes*

Principal component analysis (PCA) was applied to the RNA-seq transcripts of all genes from Exp-B (B-24% and B-72%) and Exp-Int (Int-0 and Int-320). The four selected treatments were separated mostly along PC1 (42.8% of the total variation) which seemed to describe the variation caused by light intensity, and along PC2 (17.4%), which described the variation caused by the blue light fraction (Fig. 8). Several flavonoid pathway genes had the highest loadings in PC2, closer to B-72%, whereas most of the ripening related genes (Ogasawara et al., 2007; Borovsky and Paran, 2008; Kim et al., 2014; Cheng et al., 2017; Hou et al., 2018) (Table S7) were located in the middle of the PCA plot, closer to B-24%. A few genes related to the regulation of ripening and senescence in pepper fruit (NCED1, NCED2, NOR and RIN) and red fruit pigmentation (CCS, PDS, LCY) showed negative loadings in PC2 indicating their lower expression levels in the B-72% fruit, which together with the results in Fig. 7 suggested that the higher blue light fraction delays some ripening related processes. The effect of B-72% on up-regulating the flavonoid genes, however, seemed to be the strongest which also suggested the high blue light fraction may have a specific

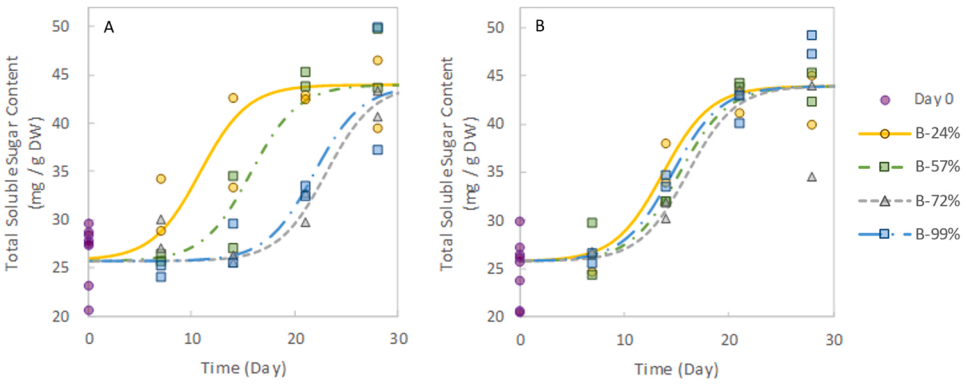

C Kinetic and ripening related parameters

	Units	Batch	Estimate	St.dev.
k_{tss}	d^{-1}		0.024	0.007
TSSmin	mg g^{-1} DW		25.8	0.4
TSSmax	mg g^{-1} DW		43.9	0.9
$shift_{24}$	d	1	10.8	1.4
$shift_{57}$	d	1	15.7	1.3
$shift_{72}$	d	1	23.0	1.3
$shift_{99}$	d	1	21.8	1.2
$shift_{24}$	d	2	13.7	1.1
$shift_{57}$	d	2	15.2	1.2
$shift_{72}$	d	2	16.0	1.3
$shift_{99}$	d	2	14.6	1.2

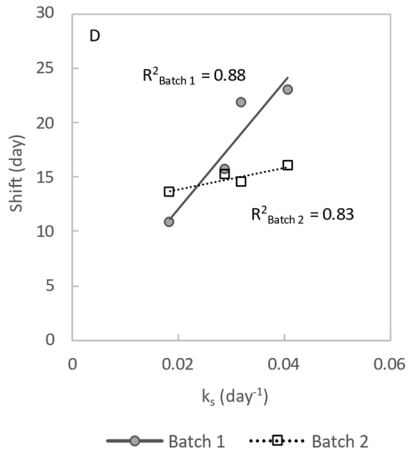

Fig. 6. Total sugar content over time either as measured values (symbols) or with simulated model behaviour (lines) for fruit in (A) batch 1 and (B) batch 2 per light treatment. (C) Parameter estimates with indicated standard deviation of the sugar model, explaining 83.5% (R^2_{adj}) of the variation (Eq. (4)). (D) The link between the anthocyanin biosynthetic rates (k_s) (Eq. (3)) and the *shift* factor, the time when the logistic curve reaches halfway the minimum and maximum TSS levels (Eq. (4)) with the explained variance per batch.

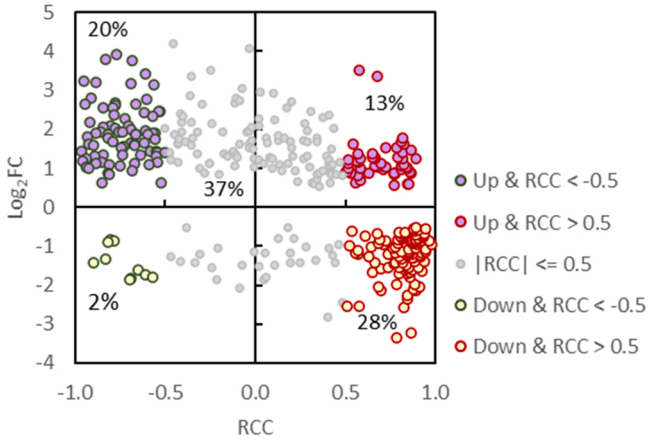

Fig. 7. The correlation between log_2 FC of DEGs of B-72% to B-24% (y-axis) at d 21 and ripening correlation coefficient (RCC) of these genes. Log_2 FC = log_2 (transcript level of genes in B-72% to B-24%). Positive Log_2 FC values indicate that genes are up-regulated in B-72% fruit whereas negative Log_2 FC values indicate that genes are down-regulated. A positive RCC values indicates genes having a high expression level in ripe fruit whereas negative RCC values indicate a high expression level in unripe fruit.

regulatory effect on the flavonoid/anthocyanin pathway.

4. Discussion

4.1. The response of anthocyanin accumulation to light intensity is minimal

Our study showed that anthocyanin content in pepper fruit was hardly affected by light intensity, including darkness (Fig. 1B). Prior studies have shown the necessity of light, and the effects of high light intensity on enhancing anthocyanin accumulation in fruit and vegetative tissues of several species (Lightbourn et al., 2007; Albert et al., 2009; Page et al., 2012; Feng et al., 2013). For example, dark-stored strawberries and Chinese bayberries had lower anthocyanin contents than illuminated fruit after several hours or days (Kadomura-Ishikawa et al., 2013; Shi et al., 2014; Xu et al., 2014). Anthocyanins did not accumulate in *Pro35S:BrTT8* tomato fruit at low-light intensity (50 – 100 μmol m^{-2} s^{-1}) (Zhang et al., 2019). Additionally, high-light-triggered anthocyanin accumulation in *Pro35S:BrTT8* tomato fruit was caused by increased expression of *SlAN2* (MYB) and anthocyanin structural genes. Albert et al. (2009) suggested that expression of *MYB* was the restricting component for producing anthocyanins under shade conditions. In our study, the slight increase of anthocyanin content of fruit from d 0 to d 7 showed that anthocyanin biosynthesis occurred during this period (Fig. 1B). However, *CaMYB* was only significantly higher expressed in darkness (Int-0) at d 7 and showed no difference among the other treatments (Fig. S1). The expression of subsequent structural genes (*CaDFR* and *CaANS*) was not influenced by light intensity (Fig. S1). Likely, light intensity only affected anthocyanin biosynthesis before d 7. Afterwards, anthocyanin biosynthesis stopped in fruit in all treatments, as inferred from the low and similar transcription levels of *CaMYB*, *CaDFR* and *CaANS*. The decrease of anthocyanin content is thus likely due to anthocyanin degradation. The anthocyanin degradation pathway could not be directly quantified because there is no identified anthocyanin degradation gene in pepper.

The highest light intensity (320 μmol m^{-2} s^{-1}) resulted in the lowest anthocyanin content during the last two weeks (Fig. 1B). This light intensity might be considered excessive. *Anthurium andraeanum* 'Sonate' leaves showed a lower anthocyanin content under excessive light (400 μmol m^{-2} s^{-1}) compared to 100 μmol m^{-2} s^{-1} (Wang et al., 2018). Excessive light may cause photodamage and oxidative stress, such as the

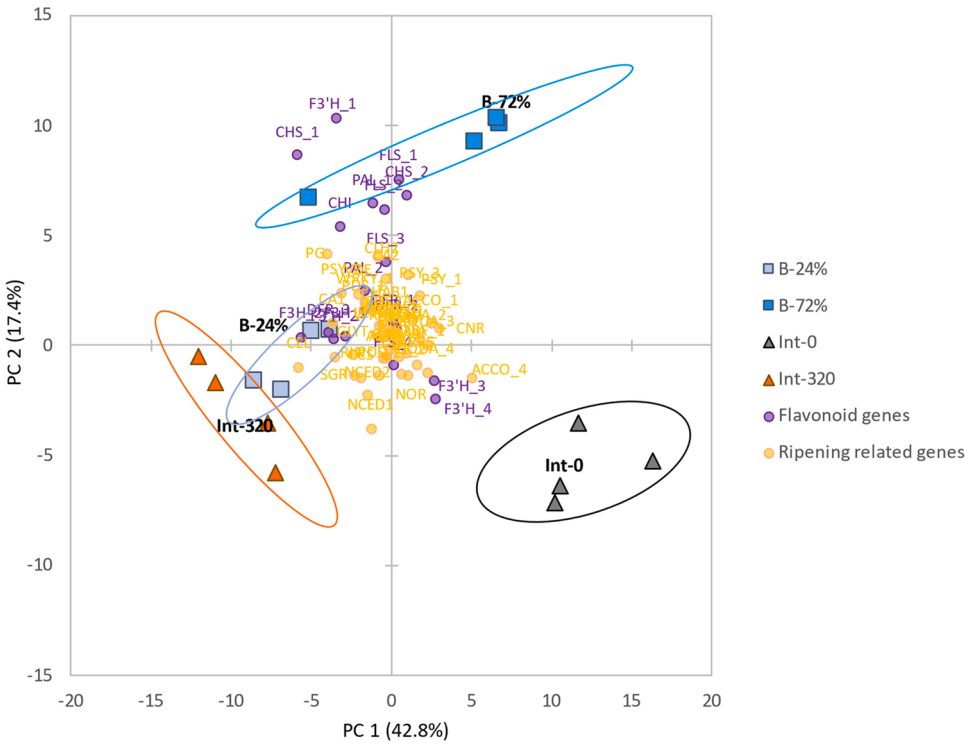

Fig. 8. Principal component analysis (PCA) of four light treatments, Int-0, Int-320, B-24% and B-72%, based on RNA-seq transcript profile (in total 9637 genes). For clarity, only the flavonoid genes and ripening related genes are displayed in this PCA plot. The PC value of each displayed gene is multiplied by 150 for easier observation. Genes with the same annotation are distinguished by their number at the end of the annotation with details provided in the Table S7.

decay of photopigments and the creation of free radicals (Lazzarin et al., 2021). In addition, water loss in fruit illuminated by 320 μmol m^{-2} s^{-1} (Fig. 1 F) reduced fruit quality and likely accelerated fruit senescence and thus indicated a potentially higher production of free radicals (Luo et al., 2014). Anthocyanins are antioxidants that help to eliminate free radicals (Li et al., 2012) and resulting in anthocyanin breakdown, this may explain the lower anthocyanin content in fruit illuminated by 320 μmol m^{-2} s^{-1}.

4.2. Higher blue light fractions enhance anthocyanin biosynthesis

Our results showed that fruit illuminated with higher fractions of blue light, especially B-72%, increased anthocyanin levels in pepper fruit compared to B-24% fruit (Fig. 2 A&B). This result is in line with the findings of Hoffmann et al. (2016) and Hernández et al. (2016) that the anthocyanin content increased with increasing fraction of blue light in pepper leaves and tomato seedlings. The anthocyanin kinetic model suggested that particularly B-72% fruit showed significantly enhanced anthocyanin biosynthesis with no effect on anthocyanin degradation (Fig. 3, Table 2). This focused our attention on anthocyanin biosynthesis. Higher expression levels of several anthocyanin biosynthetic genes (*CaMYB*, *CaDFR*, *CaANS* and *CaUFGT*) in B-72% and B-99% fruit compared to B-24% fruit showed that the anthocyanin biosynthetic pathway was enhanced with increasing fractions of blue light only during the first week (Fig. 4 A, C, D & E, Fig. S5) via stimulating the flavonoid biosynthetic pathway. The flavonoid early biosynthetic gene *CaCHS* was continuously expressed, but at varying levels, during 28 d (Fig. 4B). In addition, a transcriptomic analysis comparing fruit at B-72% to B-24% on d 21 showed that the Go term "flavonoid biosynthesis process" was enriched in the DEGs (Fig. 5 A), and that the KEGG pathway term "flavonoid biosynthesis" was enriched in B-72% up-regulated DEGs (Fig. 5B). These results demonstrated that the flavonoid biosynthetic pathway is enhanced by higher blue light fractions and it appears to be active longer than its anthocyanin branch. In addition, PCA analysis showed that early flavonoid biosynthetic genes were plotted close to fruit illuminated by 72% blue light (B-72%) but not to fruit either stored in darkness (Int-0) or illuminated by 320 μmol m^{-2} s^{-1} (Int-320) (Fig. 8). This suggests that flavonoid biosynthesis was more influenced by blue light fraction rather than by light intensity. We hypothesize that the blue light fraction affects anthocyanin biosynthesis by increasing the flux through the flavonoid pathway, leading to increased levels of anthocyanins as well as other flavonoids.

4.3. Higher blue light fractions delay pepper fruit ripening

In our study, fruit ripening was not much influenced by light intensity, unless fruit were kept in complete darkness (Fig. 1 A, C, D & E). Higher blue light fractions delayed several ripening-related processes in pepper fruit. This indicated pepper fruit ripening is more influenced by spectrum than intensity. For instance, higher blue light fractions slowed down chlorophyll breakdown and slowed down red fruit colour formation (Fig. 2 A & C). The latter was mainly due to retention of chlorophylls and anthocyanins rather than to a reduction in the red pigments as capsanthin content was not significantly affected by blue light (Fig. 2D), contrary to previous studies (Gangadhar et al., 2012; Pola et al., 2020). The sugar model indicated that the blue light fraction affected the time before sugar accumulation started, with a longer delay for fruit illuminated by higher blue light fractions (Fig. 6A-C). Soluble sugar accumulation over time in pepper fruit has been observed in pepper before (Rao et al., 2011). Likely, sugar accumulation was due to photosynthetically active chlorophyll (Cocaliadis et al., 2014; Simkin et al., 2020). Interestingly, the fastest chlorophyll breakdown was encountered in B-24% fruit (Fig. 2 C) that showed the shortest delay in sugar accumulation (Fig. 6). Furthermore, the expression pattern of ripening associated DEGs also indicated that B-72% fruit were less ripe than B-24% fruit (Fig. 7). In addition, PCA analysis showed that ripening related genes were plotted closer to fruit illuminated by 24% blue light (B-24%) than 72% blue light (B-72%) (Fig. 8). We also found that the

anthocyanin biosynthetic rate was positively correlated with the delay before total soluble sugar accumulation started (Fig. 6D), suggesting a higher anthocyanin biosynthetic rate in less ripe fruit. Thus, anthocyanin biosynthesis is strongly related to fruit ripening under varying fractions of blue light. This limits the possibility of creating ripe anthocyanin-rich fruit using light intensity or blue light treatments. One option to increase anthocyanin levels could be to use End-of-Production illumination, either ultraviolet or blue radiation, a few days before harvest as has been applied in lettuce (Gómez and Jiménez, 2020). Another option would be to apply blue or ultraviolet postharvest illumination, not continuously as was done here, but only for a few days after harvest. How this would affect the ripening characteristics of pepper fruit is currently unknown.

4.4. Higher blue fractions delay pepper ripening by lowering ethylene production?

Among enriched KEGG pathways, "sulfur metabolism" and "cysteine and methionine metabolism" were down-regulated in B-72% fruit compared to B-24% fruit (Fig. 5B). The "sulfur metabolism" was also enriched in strawberry fruit under similar conditions (Zhang et al., 2018). The "sulfur metabolism" and "cysteine and methionine metabolism" pathways are linked and present upstream of ethylene production (De Kok, 2012). *Capsicum* fruit is considered non-climacteric but climacteric behaviour has been reported in some cultivars during fruit ripening, indicating parts of the ethylene pathway may be functional (Dubey et al., 2019). For instance, cysteine and methionine, two compounds involved in the ethylene production, gradually increased during fruit ripening of bell pepper (*C. annuum* L.cv. Aries) (Aizat et al., 2014). Sole blue LED light delayed tomato fruit ripening by reducing ethylene production, compared to sole red LED light as well as mixed red and blue (R:B = 3:1) illumination (Li et al., 2021). Therefore, we hypothesize that higher blue light fraction delays pepper fruit ripening by down-regulating ethylene production. Nevertheless, the effect of blue light on fruit ripening is controversial. Ethylene production in non-climacteric fruit, such as strawberries and citrus, increased by sole blue LED illumination (Xu et al., 2014; Ballester and Lafuente, 2017). The controversial nature of the effects of blue light on ripening is also present in climacteric fruit. Sole or supplemental blue LED light illumination accelerated ripening of tomato, banana and peach (Gong et al., 2015; Huang et al., 2018; Xie et al., 2019) but slowed down ripening of tomato (Dhakal and Baek, 2014; Li et al., 2021), or did not influence ripening of tomato and blueberry (Ntagkas et al., 2020; Wang et al., 2020).

5. Conclusions

The response of purple pepper fruit to different white-red light intensities is limited with regard to anthocyanin accumulation. High blue light fractions increased anthocyanin levels via directly up-regulating anthocyanin biosynthesis and by slowing down several fruit ripening-related processes, as indicated by kinetic modelling of the sugar accumulation and transcriptome analysis, likely due to suppressed ethylene production. Higher fractions of blue light during postharvest storage can be applied to improve fruit anthocyanin levels. However, white-red light intensity or blue light treatments are not suited to create ripe anthocyanin rich pepper fruit. For future study, we suggest to apply higher fraction of blue light at the early postharvest stage or as End-of-Production illumination.

Funding

YL is financially supported by the China Scholarship Council (CSC) [grant number 201607720005] and BASF Vegetable Seeds.

CRediT authorship contribution statement

Ying Liu, Rob E. Schouten and Leo F.M. Marcelis conceptualised the research plan. Ying Liu designed the experiments, Rob E. Schouten and Leo F.M. Marcelis guided the experimental design. Ying Liu and Xinxuan Liu conducted the blue light fraction experiment and analysed the data. Ying Liu, Fei Tan and Xinxuan Liu conducted the light intensity experiment and analysed the data. Yury Tikunov mapped RNA-seq reads and performed data normalization. Rob E. Schouten performed kinetic modelling. Ying Liu wrote the manuscript except for the modelling part, and Rob E. Schouten wrote the modelling part. Rob E. Schouten, Leo F. M. Marcelis, Yury Tikunov, Arnaud Bovy and Richard G.F. Visser critically reviewed and edited the manuscript. All authors reviewed and approved the final manuscript.

Declaration of Competing Interest

The authors declare that they have no known competing financial interests or personal relationships that could have appeared to influence the work reported in this paper.

Acknowledgements

The authors would like to thank Sunrise Pepper Growers for providing pepper fruit. We thank Elias Kaiser and Nikolaos Ntagkas for their advice on experimental design; Ep Heuvelink for his guide on statistical analysis; Wei Xiong for his help on RNA-seq analysis; Jos Molthoff for his assistance in molecular work; Arjen van de Peppel for his assistance in carbohydrate analysis; Gerrit Stunnenberg, Taede Stoker and David Brink for their technical support in climate chambers. We also thank Hua Li, Dorthe Larsen, Qianxixi Min and Yongran Ji for their inspiring discussions and suggestions.

Appendix A. Supporting information

Supplementary data associated with this article can be found in the online version at doi:10.1016/j.postharvbio.2022.112024.

References

Aizat, W.M., Dias, D.A., Stangoulis, J.C.R., Able, J.A., Roessner, U., Able, A.J., 2014. Metabolomics of capsicum ripening reveals modification of the ethylene related-pathway and carbon metabolism. Postharvest Biol. Technol. 89, 19–31. https://doi.org/10.1016/j.postharvbio.2013.11.004.

Albert, N.W., Lewis, D.H., Zhang, H., Irving, L.J., Jameson, P.E., Davies, K.M., 2009. Light-induced vegetative anthocyanin pigmentation in Petunia. J. Exp. Bot. 60, 2191–2202. https://doi.org/10.1093/jxb/erp097.

Ballester, A.R., Lafuente, M.T., 2017. LED Blue Light-induced changes in phenolics and ethylene in citrus fruit: Implication in elicited resistance against Penicillium digitatum infection. Food Chem. 218, 575–583. https://doi.org/10.1016/j.foodchem.2016.09.089.

Barbagallo, R.N., Palmeri, R., Fabiano, S., Rapisarda, P., Spagna, G., 2007. Characteristic of β-glucosidase from Sicilian blood oranges in relation to anthocyanin degradation. Enzym. Microb. Technol. 41, 570–575. https://doi.org/10.1016/j.enzmictec.2007.05.006.

Borovsky, Y., Oren-Shamir, M., Ovadia, R., De Jong, W., Paran, I., 2004. The A locus that controls anthocyanin accumulation in pepper encodes a MYB transcription factor homologous to Anthocyanin2 of Petunia. Theor. Appl. Genet. 109, 23–29. https://doi.org/10.1007/s00122-004-1625-9.

Borovsky, Y., Paran, I., 2008. Chlorophyll breakdown during pepper fruit ripening in the chlorophyll retainer mutation is impaired at the homolog of the senescence-inducible stay-green gene. Theor. Appl. Genet. 117, 235–240. https://doi.org/10.1007/s00122-008-0768-5.

Chalker-Scott, L., 1999. Environmental significance of anthocyanins in plant stress responses. Photochem. Photobiol. 70, 1–9. https://doi.org/10.1111/j.1751-1097.1999.tb01944.x.

Cheng, Y., Ahammed, G.J., Yu, J., Yao, Z., Ruan, M., Ye, Q., Li, Z., Wang, R., Feng, K., Zhou, G., Yang, Y., Diao, W., Wan, H., 2017. Corrigendum: Putative WRKYs associated with regulation of fruit ripening revealed by detailed expression analysis of the WRKY gene family in pepper. Sci. Rep. 7, 43498. https://doi.org/10.1038/srep43498.

Cocaliadis, M.F., Fernández-Muñoz, R., Pons, C., Orzaez, D., Granell, A., 2014. Increasing tomato fruit quality by enhancing fruit chloroplast function. A double-edged sword. J. Exp. Bot. 65, 4589–4598. https://doi.org/10.1093/jxb/eru165.

Colanero, S., Perata, P., Gonzali, S., 2020. What's behind purple tomatoes? Insight into the mechanisms of anthocyanin synthesis in tomato fruits. Plant Physiol. 182, 1841–1853. https://doi.org/10.1104/PP.19.01530.

De Kok, L.J., 2012. Sulfate Uptake and Assimilation - Whole Plant Regulation. Sulfur metabolism in plants: mechanisms and applications to food security and responses to climate change. Springer,, Dordrecht, pp. 11–24. https://doi.org/10.1007/978-94-007-4450-9.

Dhakal, R., Baek, K.H., 2014. Short period irradiation of single blue wavelength light extends the storage period of mature green tomatoes. Postharvest Biol. Technol. 90, 73–77. https://doi.org/10.1016/j.postharvbio.2013.12.007.

Dong, B., Luo, H., Liu, B., Li, W., Ou, S., Wu, Y., Zhang, X., Pang, X., Zhang, Z., 2019. BcXyl, a β-xylosidase Isolated from Brunfelsia Calycina Flowers with Anthocyanin-β-glycosidase Activity. Int. J. Mol. Sci. 20, 1423. https://doi.org/10.3390/ijms20061423.

Du, Z., Zhou, X., Ling, Y., Zhang, Z., Su, Z., 2010. agriGO: A GO analysis toolkit for the agricultural community. Nucleic Acids Res. 38, W64–W70. https://doi.org/10.1093/nar/gkq310.

Dubey, M., Jaiswal, V., Rawoof, A., Kumar, A., Nitin, M., Chhapekar, S.S., Kumar, N., Ahmad, I., Islam, K., Brahma, V., Ramchiary, N., 2019. Identification of genes involved in fruit development/ripening in Capsicum and development of functional markers. Genomics 111, 1913–1922. https://doi.org/10.1016/j.ygeno.2019.01.002.

Fang, F., Zhang, X.L., Luo, H.H., Zhou, J.J., Gong, Y.H., Li, W.J., Shi, Z.W., He, Q., Wu, Q., Li, L., Jiang, L.L., Cai, Z.G., Oren-Shamir, M., Zhang, Z.Q., Pang, X.Q., 2015. An Intracellular Laccase Is Responsible for Epicatechin-Mediated Anthocyanin Degradation in Litchi Fruit Pericarp. Plant Physiol. 169, 2391–2408. https://doi.org/10.1104/pp.15.00359.

Feng, F.J., Li, M.J., Ma, F.W., Cheng, L.L., 2013. Phenylpropanoid metabolites and expression of key genes involved in anthocyanin biosynthesis in the shaded peel of apple fruit in response to sun exposure. Plant Physiol. Biochem. 69, 54–61. https://doi.org/10.1016/j.plaphy.2013.04.020.

Gangadhar, B.H., Mishra, R.K., Pandian, G., Park, S.W., 2012. Comparative study of color, pungency, and biochemical composition in chili pepper (Capsicum annuum) under different light-emitting diode treatments. Hortscience 47, 1729–1735. https://doi.org/10.21273/Hortsci.47.12.1729.

Gomez, C., Jimenez, J., 2020. Effect of end-of-production high-energy radiation on nutritional quality of indoor-grown red-leaf lettuce. Hortscience 55, 1055–1060. https://doi.org/10.21273/Hortsci15030-20.

Gong, D., Cao, S., Sheng, T., Shao, J., Song, C., Wo, F., Chen, W., Yang, Z., 2015. Effect of blue light on ethylene biosynthesis, signalling and fruit ripening in postharvest peaches. Sci. Hortic. 197, 657–664. https://doi.org/10.1016/j.scienta.2015.10.034.

Gould, K.S., McKelvie, J., Markham, K.R., 2002. Do anthocyanins function as antioxidants in leaves? Imaging of H2O2 in red and green leaves after mechanical injury. Plant, Cell Environ. 25, 1261–1269. https://doi.org/10.1046/j.1365-3040.2002.00905.x.

Guidi, L., Penella, C., Landi, M., 2014. Anthocyanins in mediterranean diet: Common and innovative sources. *In* Handbook of Anthocyanins: Food Sources. Chemical Applications and Health Benefits. Nova Science Publishers, Inc,, pp. 1–49. ISBN: 978-163321795-9; 978-163321762-1.

Heber, D., Bowerman, S., 2001. Applying science to changing dietary patterns. J. Nutr. 131, 3078s–3081s. https://doi.org/10.1093/jn/131.11.3078S.

Hernández, R., Eguchi, T., Deveci, M., Kubota, C., 2016. Tomato seedling physiological responses under different percentages of blue and red photon flux ratios using LEDs and cool white fluorescent lamps. Sci. Hortic. 213, 270–280. https://doi.org/10.1016/j.scienta.2016.11.005.

Hoffmann, A.M., Noga, G., Hunsche, M., 2016. Alternating high and low intensity of blue light affects PSII photochemistry and raises the contents of carotenoids and anthocyanins in pepper leaves. Plant Growth Regul. 79, 275–285. https://doi.org/10.1007/s10725-015-0132-0.

Hornero-Mendez, D., de Guevara, R.G.L., Minguez-Mosquera, M.I., 2000. Carotenoid biosynthesis changes in five red pepper (Capsicum annuum L.) cultivars during ripening. Cultivar selection for breeding. J. Agric. Food Chem. 48, 3857–3864. https://doi.org/10.1021/jf991020r.

Hou, B.Z., Li, C.L., Han, Y.Y., Shen, Y.Y., 2018. Characterization of the hot pepper (Capsicum frutescens) fruit ripening regulated by ethylene and ABA. BMC Plant Biol. 18, 162. https://doi.org/10.1186/s12870-018-1377-3.

Howard, L.R., Talcott, S.T., Brenes, C.H., Villalon, B., 2000. Changes in phytochemical and antioxidant activity of selected pepper cultivars (Capsicum species) as influenced by maturity. J. Agric. Food Chem. 48, 1713–1720. https://doi.org/10.1021/jf990916t.

Huang, J.Y., Xu, F., Zhou, W., 2018. Effect of LED irradiation on the ripening and nutritional quality of postharvest banana fruit. J. Sci. Food Agric. 98, 5486–5493. https://doi.org/10.1002/jsfa.9093.

Igwe, E.O., Charlton, K.E., Probst, Y.C., Kent, K., Netzel, M.E., 2019. A systematic literature review of the effect of anthocyanins on gut microbiota populations. J. Hum. Nutr. Diet. 32, 53–62. https://doi.org/10.1111/jhn.12582.

Jian, W., Cao, H., Yuan, S., Liu, Y., Lu, J., Lu, W., Li, N., Wang, J., Zou, J., Tang, N., Xu, C., Cheng, Y., Gao, Y., Xi, W., Bouzayen, M., Li, Z., 2019. SlMYB75, an MYB-type transcription factor, promotes anthocyanin accumulation and enhances volatile aroma production in tomato fruits. Hortic. Res. 6, 22. https://doi.org/10.1038/s41438-018-0098-y.

Kadomura-Ishikawa, Y., Miyawaki, K., Noji, S., Takahashi, A., 2013. Phototropin 2 is involved in blue light-induced anthocyanin accumulation in Fragaria x ananassa fruits. J. Plant Res 126, 847–857. https://doi.org/10.1007/s10265-013-0582-2.

Kiferle, C., Fantini, E., Bassolino, L., Povero, G., Spelt, C., Buti, S., Giuliano, G., Quattrocchio, F., Koes, R., Perata, P., Gonzali, S., 2015. Tomato R2R3-MYB Proteins SlANT1 and SlAN2: Same Protein Activity, Different Roles. Plos One 10, e0136365. https://doi.org/10.1371/journal.pone.0136365.

Kim, S., Park, M., Yeom, S.I., Kim, Y.M., Lee, J.M., Lee, H.A., Seo, E., Choi, J., Cheong, K., Kim, K.T., Jung, K., Lee, G.W., Oh, S.K., Bae, C., Kim, S.B., Lee, H.Y., Kim, S.Y., Kim, M.S., Kang, B.C., Jo, Y.D., Yang, H.B., Jeong, H.J., Kang, W.H., Kwon, J.K., Shin, C., Lim, J.Y., Park, J.H., Huh, J.H., Kim, J.S., Kim, B.D., Cohen, O., Paran, I., Suh, M.C., Lee, S.B., Kim, Y.K., Shin, Y., Noh, S.J., Park, J., Seo, Y.S., Kwon, S.Y., Kim, H.A., Park, J.M., Kim, H.J., Choi, S.B., Bosland, P.W., Reeves, G., Jo, S.H., Lee, B.W., Cho, H.T., Choi, H.S., Lee, M.S., Yu, Y., Do Choi, Y., Park, B.S., Van Deynze, A., Ashrafi, H., Hill, T., Kim, W.T., Pai, H.S., Ahn, H.K., Yeam, I., Giovannoni, J.J., Rose, J.K.C., Sørensen, I., Lee, S.J., Kim, R.W., Choi, I.Y., Choi, B.S., Lim, J.S., Lee, Y.H., Choi, D., 2014. Genome sequence of the hot pepper provides insights into the evolution of pungency in Capsicum species. Nat. Genet. 46, 270–278. https://doi.org/10.1038/ng.2877.

Kubasek, W.L., Shirley, B.W., McKillop, A., Goodman, H.M., Briggs, W., Ausubel, F.M., 1992. Regulation of flavonoid biosynthetic genes in germinating arabidopsis seedlings. Plant Cell 4, 1229. https://doi.org/10.1105/tpc.4.10.1229.

Lazzarin, M., Meisenburg, M., Meijer, D., van Ieperen, W., Marcelis, L.F.M., Kappers, I.F., van der Krol, A.R., van Loon, J.J.A., Dicke, M., 2021. LEDs Make It Resilient: Effects on Plant Growth and Defense. Trends Plant Sci. 26, 496–508. https://doi.org/10.1016/j.tplants.2020.11.013.

Li, H., Deng, Z., Zhu, H., Hu, C., Liu, R., Young, J.C., Tsao, R., 2012. Highly pigmented vegetables: Anthocyanin compositions and their role in antioxidant activities. Food Res. Int. 46, 250–259. https://doi.org/10.1016/j.foodres.2011.12.014.

Li, Q., Kubota, C., 2009. Effects of supplemental light quality on growth and phytochemicals of baby leaf lettuce. Environ. Exp. Bot. 67, 59–64. https://doi.org/10.1016/j.envexpbot.2009.06.011.

Li, Y., Liu, C., Shi, Q., Yang, F., Wei, M., 2021. Mixed red and blue light promotes ripening and improves quality of tomato fruit by influencing melatonin content. Environ. Exp. Bot. 185, 104407 https://doi.org/10.1016/j.envexpbot.2021.104407.

Lightbourn, G.J., Griesbach, R.J., Novotny, J.A., Clevidence, B.A., Rao, D.D., Stommel, J. R., 2008. Effects of anthocyanin and carotenoid combinations on foliage and immature fruit color of Capsicum annuum L. J. Hered. 99, 105–111. https://doi.org/10.1093/jhered/esm108.

Lightbourn, G.J., Stommel, J.R., Griesbach, R.J., 2007. Epistatic interactions influencing anthocyanin gene expression in Capsicum annuum. J. Am. Soc. Hortic. Sci. 132, 824–829. https://doi.org/10.21273/JASHS.132.6.824.

Liu, C.C., Chi, C., Jin, L.J., Zhu, J., Yu, J.Q., Zhou, Y.H., 2018a. The bZip transcription factor HY5 mediates CRY1a-induced anthocyanin biosynthesis in tomato. Plant Cell Environ. 41, 1762–1775. https://doi.org/10.1111/pce.13171.

Liu, F., Yu, H., Deng, Y., Zheng, J., Liu, M., Ou, L., Yang, B., Dai, X., Ma, Y., Feng, S., He, S., Li, X., Zhang, Z., Chen, W., Zhou, S., Chen, R., Liu, M., Yang, S., Wei, R., Li, H., Li, F., Ouyang, B., Zou, X., 2017. PepperHub, an Informatics Hub for the Chili Pepper Research Community. Mol. Plant 10, 1129–1132. https://doi.org/10.1016/j.molp.2017.03.005.

Liu, Y., Lv, J., Liu, Z., Wang, J., Yang, B., Chen, W., Ou, L., Dai, X., Zhang, Z., Zou, X., 2020. Integrative analysis of metabolome and transcriptome reveals the mechanism of color formation in pepper fruit (Capsicum annuum L.). Food Chem. 306, 125629 https://doi.org/10.1016/j.foodchem.2019.125629.

Liu, Y., Tikunov, Y., Schouten, R.E., Marcelis, L.F.M., Visser, R.G.F., Bovy, A., 2018b. Anthocyanin Biosynthesis and Degradation Mechanisms in Solanaceous Vegetables: A Review. Front. Chem. 6, 52. https://doi.org/10.3389/fchem.2018.00052.

Livak, K.J., Schmittgen, T.D., 2001. Analysis of relative gene expression data using real-time quantitative PCR and the 2-ΔΔCT method. Methods 25, 402–408. https://doi.org/10.1006/meth.2001.1262.

Luo, H., Dai, S.J., Ren, J., Zhang, C.X., Ding, Y., Li, Z., Sun, Y., Ji, K., Wang, Y., Li, Q., Chen, P., Duan, C., Wang, Y., Leng, P., 2014. The role of ABA in the maturation and postharvest life of a nonclimacteric sweet cherry fruit. J. Plant Growth Regul. 33, 373–383. https://doi.org/10.1007/s00344-013-9388-7.

Meng, X.C., Xing, T., Wang, X.J., 2004. The role of light in the regulation of anthocyanin accumulation in Gerbera hybrida. Plant Growth Regul. 44, 243–250. https://doi.org/10.1007/s10725-004-4454-6.

Min, Q., Marcelis, L.F.M., Nicole, C.C.S., Woltering, E.J., 2021. High Light Intensity Applied Shortly Before Harvest Improves Lettuce Nutritional Quality and Extends the Shelf Life. Front. Plant Sci. 12, 76. https://doi.org/10.3389/fpls.2021.615355.

Nakabayashi, R., Yonekura-Sakakibara, K., Urano, K., Suzuki, M., Yamada, Y., Nishizawa, T., Matsuda, F., Kojima, M., Sakakibara, H., Shinozaki, K., Michael, A.J., Tohge, T., Yamazaki, M., Saito, K., 2014. Enhancement of oxidative and drought tolerance in Arabidopsis by overaccumulation of antioxidant flavonoids. Plant J. 77, 367–379. https://doi.org/10.1111/tpj.12388.

Ntagkas, N., de Vos, R.C.H., Woltering, E.J., Nicole, C.C.S., Labrie, C., Marcelis, L.F.M., 2020. Modulation of the tomato fruit metabolome by LED light. Metabolites 10, 1–19. https://doi.org/10.3390/metabo10060266.

Ogasawara, S., Abe, K., Nakajima, T., 2007. Pepper beta-galactosidase 1 (PBG1) plays a significant role in fruit ripening in bell pepper (Capsicum annuum). Biosci. Biotechnol. Biochem. 71, 309–322. https://doi.org/10.1271/bbb.60179.

Oren-Shamir, M., 2009. Does anthocyanin degradation play a significant role in determining pigment concentration in plants? Plant Sci. 177, 310–316. https://doi.org/10.1016/j.plantsci.2009.06.015.

Page, M., Sultana, N., Paszkiewicz, K., Florance, H., Smirnoff, N., 2012. The influence of ascorbate on anthocyanin accumulation during high light acclimation in Arabidopsis thaliana: further evidence for redox control of anthocyanin synthesis. Plant Cell Environ. 35, 388–404. https://doi.org/10.1111/j.1365-3040.2011.02369.x.

Passeri, V., Koes, R., Quattrocchio, F.M., 2016. New challenges for the design of high value plant products: stabilization of anthocyanins in plant vacuoles. Front. Plant Sci. 7, 153. https://doi.org/10.3389/Fpls.2016.00153.

Pola, W., Sugaya, S., Photchanachai, S., 2020. Color development and phytochemical changes in mature green chili (Capsicum annuum L.) exposed to red and blue light-emitting diodes. J. Agric. Food Chem. 68, 59–66. https://doi.org/10.1021/acs.jafc.9b04918.

Ramakers, C., Ruijter, J.M., Deprez, R.H., Moorman, A.F., 2003. Assumption-free analysis of quantitative real-time polymerase chain reaction (PCR) data. Neurosci. Lett. 339, 62–66. https://doi.org/10.1016/s0304-3940(02)01423-4.

Rao, T.V.R., Gol, N.B., Shah, K.K., 2011. Effect of postharvest treatments and storage temperatures on the quality and shelf life of sweet pepper (Capsicum annum L.). Sci. Hortic. 132, 18–26. https://doi.org/10.1016/j.scienta.2011.09.032.

Russo, V.M., Howard, L.R., 2002. Carotenoids in pungent and non-pungent peppers at various developmental stages grown in the field and glasshouse. J. Sci. Food Agric. 82, 615–624. https://doi.org/10.1002/jsfa.1099.

Sager, J.C., Smith, W.O., Edwards, J.L., Cyr, K.L., 1988. Photosynthetic efficiency and phytochrome photoequilibria determination using spectral data. Trans. Am. Soc. Agric. Eng. 31, 1882–1889. https://doi.org/10.13031/2013.30952.

Sandoval-Ramírez, B.A., Catalán, Ú., Fernández-Castillejo, S., Rubió, L., Macià, A., Solà, R., 2018. Anthocyanin Tissue Bioavailability in Animals: Possible Implications for Human Health. A Systematic Review. J. Agric. Food Chem. 66, 11531–11543. https://doi.org/10.1021/acs.jafc.8b04014.

Schouten, R.E., Huijben, T.P.M., Tijskens, L.M.M., van Kooten, O., 2007. Modelling quality attributes of truss tomatoes: Linking colour and firmness maturity. Postharvest Biol. Technol. 45, 298–306. https://doi.org/10.1016/j.postharvbio.2007.03.011.

Shi, L., Cao, S., Chen, W., Yang, Z., 2014. Blue light induced anthocyanin accumulation and expression of associated genes in Chinese bayberry fruit. Sci. Hortic. 179, 98–102. https://doi.org/10.1016/j.scienta.2014.09.022.

Simkin, A.J., Faralli, M., Ramamoorthy, S., Lawson, T., 2020. Photosynthesis in non-foliar tissues: implications for yield. Plant J. 101, 1001–1015. https://doi.org/10.1111/tpj.14633.

Tao, R., Bai, S., Ni, J., Yang, Q., Zhao, Y., Teng, Y., 2018. The blue light signal transduction pathway is involved in anthocyanin accumulation in 'Red Zaosu' pear. Planta 248, 37–48. https://doi.org/10.1007/s00425-018-2877-y.

Tian, T., Liu, Y., Yan, H., You, Q., Yi, X., Du, Z., Xu, W., Su, Z., 2017. AgriGO v2.0: A GO analysis toolkit for the agricultural community, 2017 update. Nucleic Acids Res. 45, W122–W129. https://doi.org/10.1093/nar/gkx382.

Tijskens, L.M.M., Konopacki, P.J., Jongbloed, G., Penchaiya, P., Schouten, R.E., 2017. Assessing biological and technical variation in destructively measured data. Postharvest Biol. Technol. 132, 31–42. https://doi.org/10.1016/j.postharvbio.2017.05.013.

Tijskens, L.M.M., Schouten, R.E., 2014. Modeling quality attributes and quality related product properties. Postharvest Handling: A Systems Approach. Elsevier Inc,, pp. 411–448. https://doi.org/10.1016/B978-0-12-408137-6.00015-6.

Wahyuni, Y., Ballester, A.R., Sudarmonowati, E., Bino, R.J., Bovy, A.G., 2011. Metabolite biodiversity in pepper (Capsicum) fruits of thirty-two diverse accessions: Variation in health-related compounds and implications for breeding. Phytochemistry 72, 1358–1370. https://doi.org/10.1016/j.phytochem.2011.03.016.

Wang, Y., Liu, S., Tian, X., Fu, Y., Jiang, X., Li, Y., Wang, G., 2018. Influence of light intensity on chloroplast development and pigment accumulation in the wild-type and etiolated mutant plants of Anthurium andraeanum "Sonate'. Plant Signal. Behav. 13, 12071. https://doi.org/10.1080/15592324.2018.1482174.

Wang, Y.W., Ludwig, H.D., Scherm, H., van Iersel, M.W., Nambeesan, S.U., 2020. Blue light does not affect fruit quality or disease development on ripe blueberry fruit during postharvest cold storage. Horticulturae 6, 1–14. https://doi.org/10.3390/horticulturae6040059.

Xie, B.X., Wei, J.J., Zhang, Y.T., Song, S.W., Su, W., Sun, G.W., Hao, Y.W., Liu, H.C., 2019. Supplemental blue and red light promote lycopene synthesis in tomato fruits. J. Integr. Agric. 18, 590–598. https://doi.org/10.1016/S2095-3119(18)62062-3.

Xie, C., Mao, X., Huang, J., Ding, Y., Wu, J., Dong, S., Kong, L., Gao, G., Li, C.Y., Wei, L., 2011. KOBAS 2.0: A web server for annotation and identification of enriched pathways and diseases. Nucleic Acids Res. 39, W316–W322. https://doi.org/10.1093/nar/gkr483.

Xu, F., Shi, L., Chen, W., Cao, S., Su, X., Yang, Z., 2014. Effect of blue light treatment on fruit quality, antioxidant enzymes and radical-scavenging activity in strawberry fruit. Sci. Hortic. 175, 181–186. https://doi.org/10.1016/j.scienta.2014.06.012.

Yamada, Y., Nakayama, M., Shibata, H., Kishimoto, S., Ikeda, T., 2019. Anthocyanin production and enzymatic degradation during the development of dark purple and lilac paprika fruit. J. Am. Soc. Hortic. Sci. 144, 329. https://doi.org/10.21273/Jashs04727-19.

Zhang, Y., Li, Y., Li, W., Hu, Z., Yu, X., Tu, Y., Zhang, M., Huang, J., Chen, G., 2019. Metabolic and molecular analysis of nonuniform anthocyanin pigmentation in tomato fruit under high light. Hortic. Res. 6, 56. https://doi.org/10.1038/s41438-019-0138-2.

Zhang, Y.T., Jiang, L.Y., Li, Y.L., Chen, Q., Ye, Y.T., Zhang, Y., Luo, Y., Sun, B., Wang, X. R., Tang, H.R., 2018. Effect of red and blue light on anthocyanin accumulation and differential gene expression in strawberry (Fragaria x ananassa). Molecules 23, 820. https://doi.org/10.3390/molecules23040820.

Zipor, G., Duarte, P., Carqueijeiro, I., Shahar, L., Ovadia, R., Teper-Bamnolker, P., Eshel, D., Levin, Y., Doron-Faigenboim, A., Sottomayor, M., Oren-Shamir, M., 2015. In planta anthocyanin degradation by a vacuolar class III peroxidase in Brunfelsia calycina flowers. N. Phytol. 205, 653–665. https://doi.org/10.1111/nph.13038.

Zoratti, L., Karppinen, K., Luengo Escobar, A., Haggman, H., Jaakola, L., 2014. Light-controlled flavonoid biosynthesis in fruits. Front. Plant Sci. 5, 534. https://doi.org/10.3389/fpls.2014.00534.